Optimal, Low-Complexity Beamforming for Discrete Phase Reconfigurable Intelligent Surfaces

Sanchez, Juan; Bengtsson, Erik L; Rusek, Fredrik; Flordelis i Minguez, José; Zhao, Kun; Tufvesson, Fredrik

Published in:
2021 IEEE Global Communications Conference, GLOBECOM 2021 - Proceedings

DOI:
10.1109/GLOBECOM46510.2021.9685226

2021

Document Version:
Peer reviewed version (aka post-print)

Optimal, Low-Complexity Beamforming for Discrete Phase Reconfigurable Intelligent Surfaces

Juan Sanchez*†, Erik Bengtsson†, Fredrik Rusek*†, Jose Flordelis†, Kun Zhao† and Fredrik Tufvesson*
*Department of Electrical and Information Technology, Lund University, Lund, Sweden
†Sony Research Center, Lund, Sweden
{juan.sanchez, fredrik.tufvesson}@eit.lth.se, {erik.bengtsson, fredrik.x.rusek, jose.flordelis, kun.1.zhao}@sony.com

***Abstract*—Reflective reconfigurable intelligent surface (RIS) technology is regarded as an innovative, cost- and power-effective solution that aims at influencing the wireless channel through controlled scattering. The technology can be realized by using metamaterials and/or resonant elements that scatter electromagnetic waves with a configurable phase shift. Most of the previous work on beamforming techniques for RIS assumes ideal hardware and, thus, continuous phase shifts. However, hardware constraints limit the phase shift resolution, manifested into the amount of discrete phase shifts that can be configured into each RIS element. This paper aims to offer a discrete phase shift beamforming algorithm for reflective RISs that targets minimization of the quantization error resulting from discretization of continuous phase shifts. The beamforming solution proves to be optimal under perfect channel knowledge for any discrete set of uniformly distributed phase shifts. The required complexity to find the optimal beamforming vector for our approach is found to be linear with the number of RIS elements, the minimum needed to obtain optimal results. Simulated behavior is validated by measurements, showing robustness against angle misalignments and distance variations.**

***Index Terms*—Reconfigurable intelligent surface, low complexity, passive beamforming, optimal beamforming, discrete phase shifts, quantization error, experimental validation.**

I. Introduction

Among all the promising candidates for beyond-5G technologies, Reconfigurable Intelligent Surface (RIS) technology shows large potential thanks to its capability of shaping the propagation environment [1]. This opens up possibilities of joint radio and channel optimization, which has the potential of bringing significant increases in experienced signal-to-noise ratio (SNR). Besides communication, some potential application examples include physical layer security, wireless power transfer, sensing and many more [2], [3].

RISs are structures comprised of massive arrangements of elements referred to as Unit Cells (UCs). They can be designed to passively reflect (reflective RIS) or transmit (transmissive RIS) in directions beyond Snell's law. In this paper we are focusing on reflective RISs, and will indistinctively call them RISs onwards. The UCs may be composed of engineered materials known as metamaterials, that manipulate the properties of impinging electromagnetic (EM) waves upon interaction [4]. UCs may also be composed of resonant elements that emulate the effect of metamaterials on EM waves. One of the EM wave properties that can be controlled with RISs is the phase of the scattered EM wave from each UC, which enables beamforming techniques. For ideal realizations of RISs with continuous phase shift beamforming, theoretical boundaries on the behavior and capabilities of the RIS technology have been defined. Several works that contribute to continuous phase shift beamforming have been published [5], [6].

However, there is the need for discrete phase shift analysis to create the connection between the ideal and the practical realizations of RISs. In a practical realization of a RIS, control bits transfer the desired phase shift that is required at each UC. There are limitations on the number of phase shifts that can be configured [4]. For the simplest case in a 1-bit phase resolution realization, coding a '0' or a '1' into a UC would correspond to phase shifts of 0 and π. Perfect phase alignment for coherent combination is not possible due to the quantization error originated from discretization of continuous phase shifts. The focus of our work is optimization of beamforming gain at the RIS in a single-user system scenario, which is closely related to reduction of the quantization error at beamforming.

Most of the prior work on discrete phase shift beamforming in single-user scenarios has shown optimal solutions to be obtained with exponential complexity [7] over the number of RIS elements, and sometimes also over the number of phase shift levels [8], due to the non-convex nature of the optimization problem. The authors in [7] present sub-optimal solutions that require linear complexity dependent on number of elements, phase shift levels and algorithm iterations. The authors in [8] present sub-optimal solutions that require linear complexity with the number of elements and exponential complexity with phase shift levels. The authors in [9] present optimal solutions with continuous phase shifts that become sub-optimal after discretization, and require linear complexity with the number of elements. The question of how to further reduce required complexity without losing optimality in the process remains open.

The present paper aims to contribute to this open question by presenting an algorithm that computes the optimal beamforming vector for any discrete phase resolution, given perfect knowledge of the wireless channel. In our theoretical work, it is assumed that the phase shift levels are uniformly distributed across $[0, 2\pi)$, every phase shift configured into the RIS has same resulting insertion loss, and interaction

This project has received funding from the European Union's EU Framework Programme for Research and Innovation Horizon 2020 under Grant Agreement No. 861222.

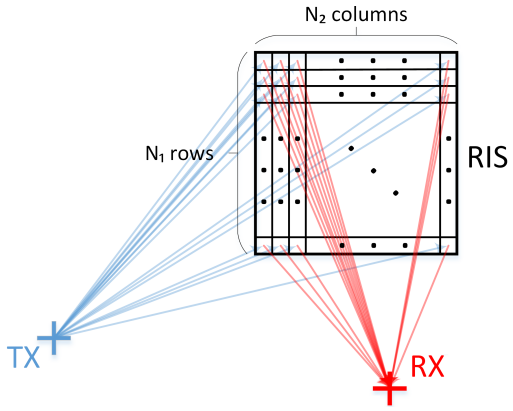

Fig. 1. RIS scenario in DL.

with impinging EM waves is independent for each UC. The optimization parameter is a joint phase shift of the wireless channel coefficients before quantization decision and discrete phase shifting, which we call quantization threshold phase (QTP). The optimal QTP, and thus the optimal beamforming vector, can be obtained with a drastic complexity reduction from the exhaustive $\mathcal{O}(2^N)$ to $\mathcal{O}(N)$ over the number of RIS elements. To validate the theoretical results we use an implementation consisting of transmit (TX) and receive (RX) horn antennas, and a RIS prototype [10] with 1-bit phase resolution. A Vector Network Analyzer (VNA) is set up to collect measurements to validate the results. The TX and RX antennas act as Base Station (BS) and User Equipment (UE), respectively, in a scenario where we study the downlink (DL) performance.

II. System Model

We consider a scenario composed of a BS, a RIS and a UE. Without loss of generality, we focus on the DL and assume channel reciprocity. Then, the BS acts as the TX, whereas the UE acts as the RX. In many application cases there is line-of-sight (LOS) between the TX and the RIS, as well as between the RIS and the RX, but no LOS between the TX and the RX, as illustrated in Fig. 1. The TX and RX are composed of a single antenna element with omnidirectional radiation pattern, whereas the RIS is an array of N_1 rows and N_2 columns, with $N = N_1 \cdot N_2$ omnidirectional UCs. In the system model, the specular path between the TX and the RX through the RIS dominates the transmission. Hence, we assume there is no non-line-of-sight (NLOS) contributions, nor large- or small-scale fading. We additionally assume no path-loss nor coupling between UCs. We start with a simple geometric, narrow-band model for the transmission between the RX and the TX through reflection at the RIS. The overall channel can be regarded as a single-input single-output (SISO) channel, whereas the channels between the RIS and the RX, and between the TX and the RIS, can be regarded as multiple-input single-output (MISO) and single-input multiple-output (SIMO) channels, respectively. At the RX side, the reflected signal via the RIS can be seen as a cluster of multi-path components (MPCs), where the geometric position of each UC determines its phase contribution. The SISO channel h can be expressed as

$$h = \mathbf{h}_{\mathrm{RX}}^{\intercal}\, \mathbf{B}\, \mathbf{h}_{\mathrm{TX}}, \tag{1}$$

where $\mathbf{h}_{\mathrm{RX}} \in \mathbb{C}^{N\times 1}$ is the MISO channel between the RIS and the RX, $\mathbf{B} \in \mathbb{C}^{N\times N}$ is the RIS response and $\mathbf{h}_{\mathrm{TX}} \in \mathbb{C}^{N\times 1}$ is the SIMO channel between the TX and the RIS. Under our assumptions, we assume we can decouple the RIS response $\mathbf{B}$ and express it as $\mathbf{B} = \mathrm{diag}\{\mathbf{b}\}$ with $\mathbf{b} \in \mathbb{C}^{N\times 1}$ representing the reconfigurable beamforming vector. The vectors $\mathbf{h}_{\mathrm{RX}}$ and $\mathbf{h}_{\mathrm{TX}}$ capture the effects of phase shift caused by the distance to the RIS. Hence, they can be expressed as

$$\mathbf{h}_{\mathrm{RX}} = \exp\left(-j2\pi f_c \frac{\mathbf{d}_{\mathrm{RX}}}{c}\right),\ \mathbf{h}_{\mathrm{TX}} = \exp\left(-j2\pi f_c \frac{\mathbf{d}_{\mathrm{TX}}}{c}\right),$$

where $\mathbf{d}_{\mathrm{RX}},\ \mathbf{d}_{\mathrm{TX}} \in \mathbb{R}^{N\times 1}$ represent distances between the RX/TX and each element from the RIS, f_c represents the carrier frequency, and c is the speed of light. By using matrix properties, (1) can be rewritten as

$$\begin{aligned} h &= \mathbf{h}_{\mathrm{RX}}^{\intercal}\mathrm{diag}\{\mathbf{b}\}\mathbf{h}_{\mathrm{TX}} \\ &= \mathbf{h}_{\mathrm{RX}}^{\intercal}(\mathbf{b}\circ\mathbf{h}_{\mathrm{TX}}) \\ &= \mathbf{b}^{\intercal}(\mathbf{h}_{\mathrm{RX}}\circ\mathbf{h}_{\mathrm{TX}}) \\ &= \mathbf{b}^{\intercal}\mathbf{g}, \end{aligned} \tag{2}$$

where $\mathbf{g} = \mathbf{h}_{\mathrm{RX}} \circ \mathbf{h}_{\mathrm{TX}} = \exp\left(-j2\pi f_c \frac{\mathbf{d}_{\mathrm{RX}} + \mathbf{d}_{\mathrm{TX}}}{c}\right)$ models the SISO channel between TX and RX without considering the decoupled RIS response. The operator $\{\circ\}$ denotes the Hadamard product. For $0 \le k \le N-1$, each element g_k can be thought of as representing a MPC, and each element b_k represents a beamforming coefficient. Hereafter, each element g_k will be referred to as a RIS path, and each element $b_k g_k$ as a beamformed RIS path.

III. Conventional Beamforming and Optimization for Practical RIS

If we want to maximize the gain at the RX based on the model in (2), coherent contribution from all RIS paths should be ensured. In other words, phase alignment for all RIS paths should be ensured. For the channel h, we can thus derive the maximum-ratio transmission (MRT) beamformer $\dot{\mathbf{b}}$ as

$$\dot{\mathbf{b}} = \exp\left(j2\pi f_c \frac{\mathbf{d}_{\mathrm{RX}} + \mathbf{d}_{\mathrm{TX}}}{c}\right). \tag{3}$$

For a theoretical RIS with countinuous phase shifts, a joint phase shift of all beamforming coefficients b_k would only cause a resulting shift in overall phase of the SISO channel h, with its magnitude left unchanged. This holds true since all the RIS paths would coherently shift in phase. However, physical properties of the metasurfaces that are typically used do not allow for continuous phase shift configuration. In fact, the elements in $\mathbf{b}$ can only take values from a restricted set of phase shifts $\mathcal{S}$. The limitation to a restricted set of discrete phase shifts inherently results in quantization of continuous

phase shifts and errors that lead to imperfect misalignment of the RIS path phases. This, in turn, causes incoherent RIS path combining and impossibility of practically realizing the MRT beamformer in (3).

The set $\mathcal{S}$ is generated by a quantization number Q that determines the amount of possible phase shifts a RIS can have. For a quantization number $Q = 2^n$, with $n \in \mathbb{N}^+$ representing the phase resolution in bits (for $n \notin \mathbb{N}^+$ there is no phase shifting possibility), we have the set $\mathcal{S}$ of all possible quantized phase shifts s as follows:

$$\mathcal{S} = \left\{ s : s = \exp\left(\frac{j2a\pi}{Q}\right), \text{ for } a = \{0, 1, \ldots, Q-1\} \right\}. \tag{4}$$

Then, the beamforming optimization problem can be formulated as

$$\max_{\mathbf{b} \in \mathcal{S}^N} \left\{ |\mathbf{b}^\intercal \mathbf{g}|^2 \right\}, \tag{5}$$

with N denoting the number of RIS elements. An exhaustive search for the optimal beamforming vector over all possible $\mathbf{b} \in \mathcal{S}^N$ would require complexity $\mathcal{O}(2^N)$. The problem presented here is a special case of a fixed-rank, convex quadratic maximization problem for discrete variables with finite number of permitted values, where the rank of $\mathbf{g}$ is 1. The authors in [11] showed that, for binary variables and fixed-rank d, the maximization problem can be solved with complexity $\mathcal{O}(N^{d-1})$ for $d \geq 3$ and $\mathcal{O}(N^d)$ for $d \leq 2$. Binary variables as in our scenario would correspond to the special case where $Q = 2$, i.e. phase shifts of 0 and π. Thus, the optimization problem in (5) for $Q = 2$ can be solved with complexity $\mathcal{O}(N)$. In an alternative approach to [11], and extending for a general Q, we can delimit our search with the following lemma.

Lemma 1. Let $\mathbf{b} \in \mathcal{S}^N$ with $\mathcal{S}$ as in (4). Let h and $\mathbf{g}$ be defined as in (2). Let us further define the function $f(x, y)$, with $x, y \in \mathbb{C}$, that calculates the internal angle between two complex values, i.e.,

$$f(x,y) = \begin{cases} |\mathrm{Arg}(y) - \mathrm{Arg}(x)|, & \text{if } |\mathrm{Arg}(y) - \mathrm{Arg}(x)| \leq \pi, \\ 2\pi - |\mathrm{Arg}(y) - \mathrm{Arg}(x)|, & \text{otherwise,} \end{cases}$$

with $\mathrm{Arg}(z) \in [-\pi, \pi)$ defining the argument of $z \in \mathbb{C}$. If $\mathbf{b}$ is optimal, i.e.

$$|h|^2 \geq \left| \hat{\mathbf{b}}^\intercal \mathbf{g} \right|^2, \ \forall \hat{\mathbf{b}} \neq \mathbf{b},$$

it always holds that

$$f(h - b_k g_k, b_k g_k) \leq \frac{\pi}{Q}, \ \forall 0 \leq k \leq N-1.$$

Proof. See Appendix A. □

Lemma 1 expresses that even though perfect phase alignment of the RIS paths is impossible to achieve in the discrete domain, there is a higher bound on the phase difference between each beamformed RIS path $b_k g_k$ and the overall SISO channel h, as a necessary condition for optimality. This implies that no beamforming vector $\mathbf{b}$ can achieve optimal combining among RIS paths for a certain h if any beamformed RIS path phase $\mathrm{Arg}(b_m g_m)$ lies outside the region defined by the number of possible quantized phase shifts in a RIS.

Since phase shifts are discrete, the joint phase shift of all beamforming coefficients b_k would come with posterior quantization and errors that result in variations in the magnitude of the SISO channel h. Let us refer to the joint phase shift of all beamforming coefficients b_k as the QTP of the beamformer φ. It becomes necessary to include the QTP when aiming to maximize the gain at the RX. More specifically, for $0 \leq \varphi \leq 2\pi$, the phase-dependent beamformer that extends (3) to the discrete domain can be expressed as

$$\mathbf{b}(\varphi) = \exp\left(j \frac{2\pi}{Q} \mathrm{round}\left(\left[f_c \frac{\mathbf{d}_{\mathrm{RX}} + \mathbf{d}_{\mathrm{TX}}}{c} + \frac{\varphi}{2\pi} \right] \cdot Q \right) \right), \tag{6}$$

where the $\mathrm{round}()$ operator approximates its argument's value to the nearest integer. For some $\varphi_1 \neq \varphi_2$, $\mathbf{b}(\varphi_1) \neq \mathbf{b}(\varphi_2)$. When $Q \to \infty$, the special case, equivalent to (3), where all possible $\mathbf{b}(\varphi)$ are optimal arises, i.e., for $0 \leq \varphi \leq 2\pi$,

$$\mathbf{b}(\varphi) = \dot{\mathbf{b}} = \exp\left(j \left(2\pi f_c \frac{\mathbf{d}_{\mathrm{RX}} + \mathbf{d}_{\mathrm{TX}}}{c} + \varphi \right) \right).$$

The discrete phase-dependent beamformer forces the phases of each RIS path g_k to align as close as possible to the overall phase of the SISO channel h, by applying discrete phase shifts b_k that take values from a set $\mathcal{S}$. The beamforming vector $\mathbf{b}(\varphi)$ is unique for each QTP φ. By varying the QTP φ, the expected phase of the SISO channel h varies too.

Theorem 1. For a given $\mathbf{g}$, as in (2), the optimal discrete beamforming vector can be computed as $\dot{\mathbf{b}} = \mathbf{b}(\dot{\varphi})$, where

$$\dot{\varphi} = \arg \max_{0 \leq \varphi \leq 2\pi} \left\{ |\mathbf{b}^\intercal(\varphi) \mathbf{g}|^2 \right\}$$

is the optimal QTP and $\mathbf{b}(\varphi) \in \mathcal{S}$ as in (6). Furthermore, $\dot{\varphi}$ can be obtained with linear complexity $\mathcal{O}(N)$.

Proof. See Appendix B. □

Maximizing $|\mathbf{b}^\intercal \mathbf{g}|^2$ over all φ ensures that, from all possible MRT beamformers $\mathbf{b}(\varphi)$, we are taking the beamforming vector $\dot{\mathbf{b}}$ that maximizes the gain when quantization error comes into the game because of the restricted set of phase shifts $\mathcal{S}$ we can apply. Since perfect RIS path phase alignment cannot be realized, the optimal discrete beamforming vector solves (5) and ensures that the RIS paths best combine given the discrete constraints. The required complexity when searching for it can be drastically reduced from $\mathcal{O}(2^N)$ in the exhaustive-search case, to $\mathcal{O}(N)$ with the result of Theorem 1. The complexity remains linear with $\mathcal{O}(N)$ even if n, and consequently Q, increase.

IV. Implementation

In this section, we describe the validation procedure for the beamforming algorithm given in Theorem 1. A MATLAB script simulating the geometrical model given in (2) was

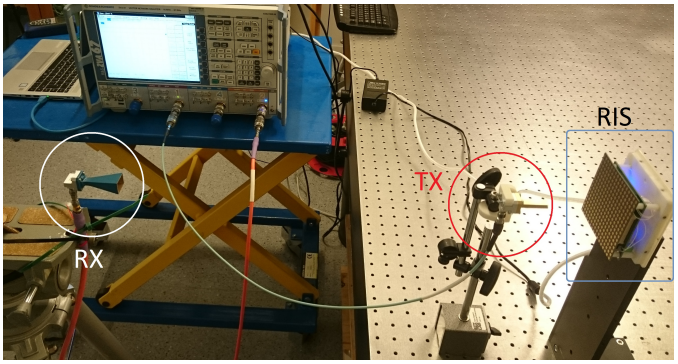

Fig. 2. Validation setup. Absorbers were removed from the scenario, and the distance between the RIS and the RX was shortened for clarity in the picture.

created. Beamforming with different initial phase shifts, according to (6), was carried out on top of the geometrical model. The resulting magnitude of the SISO channel h was evaluated against the QTP. To test the RIS beamforming algorithm and see how well it adjusts to reality, a DL SISO scenario was set up. It consisted of two horn antennas and one RIS [10], as shown in Fig. 2. The RIS had 1-bit phase resolution and its two possible phase shift levels had a phase difference of 180°. Range measurements were carried out with a precision of 1 mm. Angular measurements were calibrated and estimated to have a tolerance of $\pm 0.5°$.

Measurements were collected with a VNA, sent through Ethernet to the computer and stored as comma-separated vector (.csv) files for post-processing in MATLAB. The horn antenna in the near field acted as TX, and was connected to Port 1 (P1) of the VNA. The antenna in the far field acted as RX, and was connected to Port 2 (P2) of the VNA. TX and RIS were in LOS, as well as RX and RIS. The TX remained static, whereas the RX was moved around in the scenario. Control of the RIS was done via Universal Serial Bus (USB) communication using Python, by using (6) with different QTPs. The complete routine enabled sweeping over all desired QTPs, and subsequent measurement of the magnitude of the S21 parameter – i.e. received power – at the VNA. All measured traces were normalized to a calibration measurement consisting of received power at 28 GHz, at boresight between TX and RIS and between RIS and RX, at QTP of 0°. The resulting normalized received power was evaluated for different QTPs, representing the gain [dB] with respect to the calibration measurement. At post-processing, the simulated trace for the received power was normalized to the measurements. The normalization factor for the simulated trace reflects the mean power of the measured trace at 28 GHz, at the corresponding angles between TX and RIS and between RIS and RX. There were 3 scenarios of interest, namely when the azimuth of departure (AOD) from the RIS to the RX was -10°, 0° and 10°. All of the scenarios followed the considerations described in Section II. All measurement parameters are summarized in Table I. The main goal of the measurements was to validate the simulated behavior of the beamforming gain upon varying the QTP, which allows to validate the optimality of the algorithm presented in Theorem 1. Also, its robustness against misalignments in angle – AOD in this case – and range was evaluated.

TABLE I
PARAMETER SETUP.

Center frequency (f_c)	28 GHz
Wavelength (λ)	10.7 mm
RIS (elements)	16×16 [10]
TX antenna	SGW PEWAN1131 6.5dBi
RX antenna	SGH PE9850/2F-15 15dBi
VNA	R&S ZVA67 10MHz-67GHz
VNA output power	10 dBm
VNA resolution bandwidth (RBW)	1 kHz
VNA average factor	20
TX-RIS range (R_{TX})	66 mm
TX-RIS elevation of arrival (EOA)	0 deg
TX-RIS azimuth of arrival (AOA)	0 deg
RIS-RX range (R_{RX})	1500 mm
RIS-RX elevation of departure (EOD)	0 deg
RIS-RX azimuth of departure (AOD)	{-10, 0, 10} deg
QTP range	[0,359] deg
QTP step	1 deg

V. RESULTS AND VERIFICATION

Fig. 3 shows gain results, in dB, as a function of the QTP, in degrees, which the beamforming vector in (6) takes as argument to align the RIS paths from the model in (2). The setup considered measurements for a physical configuration with boresight in azimuth and elevation for TX and RIS, and for RIS and RX, at a range of 66 mm ($\sim 6.2\lambda$) between TX and RIS, and 1500 mm ($\sim 140.1\lambda$) between RIS and RX. The configuration of the beamforming algorithm matched the ranges between components, and varied the AOD between -4° and 4°, so that the effect of angle misalignment could be measured in the setup. The blue and orange traces are highlighted in the plot. They represent the simulated and measured traces, respectively, for the configuration of the beamforming algorithm that matched the ranges and angles between the components. Since the RIS UCs for this specific implementation were found to have different insertion loss depending on their phase shift state – ∼3 dB difference, simulations were adjusted to include its effect on the gain. Additionally, misalignments that recreate a more realistic imprecise scenario were added to the simulation. The traces' overall behaviors with respect to QTP agree, and further simulations show that neglecting the pathloss in the computation does not seem to have a noticeable degrading effect. For the simulated trace in blue, an increase in imprecisions correlates with either more pronounced variations or shape alterations. From the measured trace in orange, it is clear that there are 2 regions, spanning 180° each, along the QTP axis. One of the regions contains a local maximum, whereas the other contains the global maximum, both of them 180° apart from each other. This is expected as the quantization number $Q = 2$ creates 2 beamforming regions, each entailing 180° intervals, that

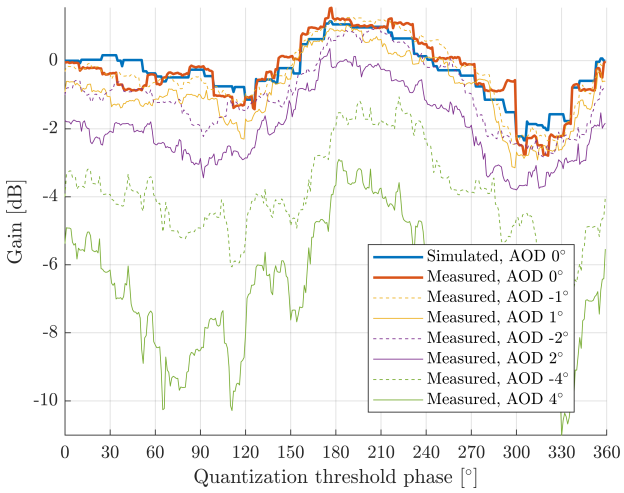

Fig. 3. Simulated and measured gain for matched beamforming configuration R_{TX} = 66 mm, R_{RX} = 1500 mm, EOA = AOA = EOD = AOD = 0°; and measured gain for deviations of beamforming AOD = $\pm\{1,2,4\}°$. For the simulated gain, angular misalignments of 3° in arrivals and 1° in departures, a range misalignment of 10mm between the TX and the RIS, and an insertion loss imbalance between UC states of 3dB, were introduced.

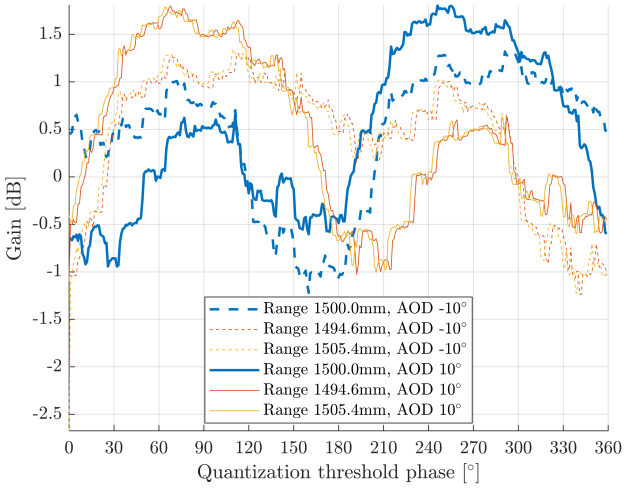

Fig. 4. Measured gain for matched beamforming configuration R_{TX} = 66 mm, R_{RX} = 1500 mm, EOA = AOA = EOD = 0°, AOD = ± 10°; and for deviations of beamforming R_{RX} = 1500.0 ± 5.4 mm.

are equivalent as long as the states of the UCs for phase shifts of 0° and 180° exhibit the same reflecting gain. The asymmetry between regions comes then from the insertion loss difference between UC states. Simulations conclude that the losses associated to one of the two states of the RIS UCs are evidenced in the measured trace in orange, that they contribute to asymmetry and more pronounced gain variations, and that its knowledge can improve discrete beamforming in a practical scenario.

The thinner traces in the plot represent the results from beamforming configurations where the RIS pointed at an AOD of $\pm\{1,2,4\}°$ deviating from the physical AOD of 0°. It is clear that bigger deviations translate into greater losses, and transmission suffers greatly from small deviations in angle. The trace for matched AOD exhibits a peak at 177° QTP. The mean loss for deviations of $\{1,2,4\}°$ is approximately $\{0.5,1.4,4.6\}$ dB. This goes in line with the observations in [12]. From here, it appears that a positioning accuracy of at least 2° is needed to mitigate beamforming losses due to misalignment. It is interesting however, that the phase-dependent behavior does not get strongly distorted, even for misalignments of 4°, preserving the peak locations in the vicinity of the optimal QTP. With this, the optimal discrete phase shift beamforming has shown to be robust under angular misalignments.

The setup in Fig. 4 considered two scenarios with physical AOD of ±10°, all of the other angles in boresight and ranges of 66 mm between TX and RIS, and of 1500 mm between RIS and RX. Dashed lines are bound to physical AOD -10°, whereas solid lines are bound to physical AOD 10°. The beamforming algorithm was adjusted to match the physical AOD for all of the traces displayed in the figure. The range between RIS and RX configured to the beamforming algorithm was of interest in this case. Misalignments of $\lambda/2$ were configured to the RIS, while keeping the physical range at 1500 mm. The highlighted traces in blue represent the cases where the beamforming algorithm was configured to match the physical distance. According to the geometrical model developed in Section II, the traces should ideally be equal, since there is symmetry for a perfectly precise setup. Inaccuracies and artifacts introduced by this specific RIS device cause them to be slightly misaligned, even though they conserve the same pattern, which also agrees with the simulated pattern for all QTPs considered. The effect of unequal insertion loss at UCs for phase shifts of 0° and 180° due to the RIS design is clearly noticed in this plot too. The orange traces illustrate the measurement results when the algorithm was configured to beamform at a misaligned range between RIS and RX of $\lambda/2$ away from the physical estimated range 1500 mm, i.e. 1505.4 mm for f_c = 28 GHz. The yellow traces illustrate the same procedure done for a misaligned range between RIS and RX of $\lambda/2$ closer, i.e. 1494.6 mm for f_c = 28 GHz. It is clear from Fig. 4 that both distance misalignments from the beamforming perspective cause a shift in measured traces of around 180°. This is expected, since the expected phase of the received signal shifts 180° with an offset of $\lambda/2$. Then, the optimal QTP where the maximum lies shifts 180° too. Notice that since the channel coefficients shift in phase at the complex plane with distance, the QTP shifts by the same proportion, conserving identical or almost identical beamforming patterns for wavelength-order distance offsets when at far-field. Symmetry upon range misalignment still holds for AOD ±10°. The curves do not match perfectly in phase, with a misalignment of 3° between beamforming ranges 1494.6 and 1505.4 mm. Here inaccuracies and artifacts influence this fact too.

VI. Conclusions

The results validate that the discrete beamforming method for RISs proposed in Theorem 1 performs optimally for any discrete set of uniformly distributed phase shifts, obtains

its solution with complexity $\mathcal{O}(N)$, and is robust against misalignments in angle as well as changes in distance. The beamforming vector calculated according to Theorem 1 can therefore work well under mild imperfections in the estimation and be used as a method for discrete beamforming upon channel feedback. Positioning accuracy of at least 2 degrees is recommended to mitigate beamforming losses due to misalignment for the tested implementation with a 16×16 RIS. It is still an open question whether the positioning accuracy requirement tightens with increasing number of RIS elements N.

Appendix A
Proof of Lemma 1 (by contradiction)

Assume $\mathbf{b}$ optimal and assume $\exists m, 0 \leq m \leq N-1$, such that

$$f(h - b_m g_m, b_m g_m) > \frac{\pi}{Q}.$$

It is clear that $|s| = 1$ and $0 \leq a \leq Q-1$, so $0 \leq a < Q$. Moreover, it is possible to prove that the set $\mathcal{S}$ is closed under multiplication. Since $\mathcal{S}$ is a closed set under multiplication, there exists a $b'_m \in \mathcal{S}$ such that $b'_m b_m \in \mathcal{S}$ and $f(h - b_m g_m, b'_m b_m g_m) \leq \pi/Q$. Now,

$$\begin{aligned}|\hat{h}|^2 &= |h - b_m g_m + b'_m b_m g_m|^2 \\ &= |h - b_m g_m|^2 + |b'_m b_m g_m|^2 \\ &\quad + 2 \cdot |h - b_m g_m|\, |b'_m b_m g_m| \\ &\quad \cos(f(h - b_m g_m, b'_m b_m g_m)).\end{aligned}$$

Notice that, for any $x, y \in \mathbb{C}$, $f(x, y) \leq \pi$. Besides, $\cos(\theta)$ is strictly decreasing for $0 \leq \theta \leq \pi$. This implies that $\cos(\theta_1) \geq cos(\theta_2)$ for $\theta_1 \leq \theta_2$, with equality iff $\theta_1 = \theta_2$. Then, we have

$$0 \leq f(h - b_m g_m, b'_m b_m g_m) \leq \frac{\pi}{Q},$$

$$\frac{\pi}{Q} < f(h - b_m g_m, b_m g_m) \leq \pi,$$

which allows us to infer that

$$1 \geq \cos(f(h - b_m g_m, b'_m b_m g_m)) \geq \cos\left(\frac{\pi}{Q}\right),$$

$$\cos\left(\frac{\pi}{Q}\right) > \cos(f(h - b_m g_m, b_m g_m)) \geq -1.$$

Developing further for $|\hat{h}|^2$, we have

$$\begin{aligned}|\hat{h}|^2 &= |h - b_m g_m|^2 + |b_m g_m|^2 + 2 \cdot |h - b_m g_m|\, |b_m g_m| \\ &\quad \cos(f(h - b_m g_m, b'_m b_m g_m)) \\ &> |h - b_m g_m|^2 + |b_m g_m|^2 + 2 \cdot |h - b_m g_m|\, |b_m g_m| \\ &\quad \cos(f(h - b_m g_m, b_m g_m)) \\ &= |h - b_m g_m + b_m g_m|^2 \\ &= |h|^2.\end{aligned}$$

Then, $\mathbf{b}$ is not optimal. But $\mathbf{b}$ was assumed to be optimal. Therefore, it must hold that

$$f(h - b_k g_k, b_k g_k) \leq \frac{\pi}{Q},\ \forall 0 \leq k \leq N-1.$$

The proof is thus completed.

Appendix B
Proof of Theorem 1

Let $h = \sum_{0 \leq k \leq N-1} b_k g_k$, with $\mathrm{Arg}(h) = \varphi$. Using Lemma 1, if $\exists m, 0 \leq m \leq N-1$, such that $f(h - b_m g_m, b_m g_m) > \frac{\pi}{Q}$, then $\mathbf{b}$ is not optimal. The beamforming vector $\mathbf{b}(\varphi)$ in (6) belongs to the set $\mathcal{S}$ and ensures that

$$f(h - b_k g_k, b_k g_k) \leq \frac{\pi}{Q},\ \forall 0 \leq k \leq N-1.$$

Therefore, the beamforming vector meets the necessary condition of optimality. It also holds that, for any $h_1 \neq h_2$, $\mathrm{Arg}(h_2) = \mathrm{Arg}(h_1) + \Delta\varphi = \varphi_1 + \Delta\varphi$. Then, computing the beamforming vector that meets the necessary condition for optimality, for all possible h, is equivalent to computing a beamforming vector that meets such condition, for all possible φ. Further considering (6), for some $\varphi_1, \varphi_2 \in [0, 2\pi)$, $b(\varphi_1) = b(\varphi_2)$. There is no need to evaluate such cases that arise when $\forall g_k,\ \mathrm{Arg}(g_k) \notin [\varphi_1, \varphi_2]$. The fact that there are N RIS paths g_k, and thus N QTPs φ that should be evaluated, ensures the computation complexity to be linear with $\mathcal{O}(N)$. The proof is thus completed.

References

[1] E. Basar, M. Di Renzo, J. De Rosny, M. Debbah, M.-S. Alouini, and R. Zhang, "Wireless communications through reconfigurable intelligent surfaces," *IEEE access*, vol. 7, pp. 116753–116773, 2019.

[2] M. Di Renzo, A. Zappone, M. Debbah, M.-S. Alouini, C. Yuen, J. de Rosny, and S. Tretyakov, "Smart radio environments empowered by reconfigurable intelligent surfaces: How it works, state of research, and the road ahead," *IEEE Journal on Selected Areas in Communications*, vol. 38, no. 11, pp. 2450–2525, 2020.

[3] Q. Wu, S. Zhang, B. Zheng, C. You, and R. Zhang, "Intelligent reflecting surface aided wireless communications: A tutorial," *IEEE Transactions on Communications*, 2021.

[4] T. J. Cui, S. Liu, and L. Zhang, "Information metamaterials and metasurfaces," *Journal of Materials Chemistry C*, vol. 5, no. 15, pp. 3644–3668, 2017.

[5] Y. Zhang, J. Zhang, M. Di Renzo, H. Xiao, and B. Ai, "Performance analysis of RIS-aided systems with practical phase shift and amplitude response," *IEEE Transactions on Vehicular Technology*, 2021.

[6] Q. Wu and R. Zhang, "Intelligent reflecting surface enhanced wireless network via joint active and passive beamforming," *IEEE Transactions on Wireless Communications*, vol. 18, no. 11, pp. 5394–5409, 2019.

[7] Q. Wu and R. Zhang, "Beamforming optimization for wireless network aided by intelligent reflecting surface with discrete phase shifts," *IEEE Transactions on Communications*, vol. 68, no. 3, pp. 1838–1851, 2019.

[8] M. Jung, W. Saad, M. Debbah, and C. S. Hong, "On the optimality of reconfigurable intelligent surfaces (RISs): Passive beamforming, modulation, and resource allocation," *IEEE Transactions on Wireless Communications*, 2021.

[9] Z. Yigit, E. Basar, and I. Altunbas, "Low complexity adaptation for reconfigurable intelligent surface-based MIMO systems," *IEEE Communications Letters*, vol. 24, no. 12, pp. 2946–2950, 2020.

[10] L. Yezhen, R. Yongli, Y. Fan, X. Shenheng, and Z. Jiannian, "A novel 28 GHz phased array antenna for 5G mobile communications," *ZTE Communications*, vol. 18, no. 3, pp. 20–25, 2020.

[11] K. Allemand, K. Fukuda, T. M. Liebling, and E. Steiner, "A polynomial case of unconstrained zero-one quadratic optimization," *Mathematical Programming*, vol. 91, no. 1, pp. 49–52, 2001.

[12] W. Tang, M. Z. Chen, X. Chen, J. Y. Dai, Y. Han, M. Di Renzo, Y. Zeng, S. Jin, Q. Cheng, and T. J. Cui, "Wireless communications with reconfigurable intelligent surface: Path loss modeling and experimental measurement," *IEEE Transactions on Wireless Communications*, 2020.